DE GRUYTER OPEN

Int. J. of Applied Mechanics and Engineering, 2016, vol.21, No.1, pp.121-141
DOI: 10.1515/ijame-2016-0008

AXISYMMETRIC MIXED CONVECTIVE MHD FLOW OVER A SLENDER CYLINDER IN THE PRESENCE OF CHEMICALLY REACTION

K.V. PRASAD* and H. VAIDYA
Department of Mathematics
Vijayanagara Sri Krishnadevaraya University
Ballari- 583104, INDIA
E-mail: prasadkv2007@gmail.com

K. VAJRAVELU
Department of Mathematics, Department of Mechanical
Materials and Aerospace Engineering, University of Central Florida
Orlando, FL 32816, USA

P.S. DATTI
TIFR Centre, IISC-TIFR Joint Programme in Applications of Mathematics
Indian Institute of Science
Bangalore, Karnataka, INDIA

V. UMESH
Department of Civil Engineering, SJB Institute of Technology
Bangalore, Karnataka, INDIA

The present analysis is focused on the study of the magnetic effect on coupled heat and mass transfer by mixed convection boundary layer flow over a slender cylinder in the presence of a chemical reaction. The buoyancy effect due to thermal diffusion and species diffusion is investigated. Employing suitable similarity transformations, the governing equations are transformed into a system of coupled non-linear ordinary differential equations and are solved numerically via the implicit, iterative, second order finite difference method. The numerical results obtained are compared with the available results in the literature for some special cases and the results are found to be in excellent agreement. The velocity, temperature, and the concentration profiles are presented graphically and analyzed for several sets of the pertinent parameters. The pooled effect of the thermal and mass Grashof number is to enhance the velocity and is quite the opposite for temperature and the concentration fields.

Key words: magnetic field, chemical reaction, heat and mass transfer, convective flow, slender cylinder, Grashof number, Keller-box method.

1. Introduction

Magnetohydrodynamic (MHD) convective flow has numerous applications in technological industry such as MHD pumps, MHD generators, magnetic suppression of molten semi conducting materials, MHD couples and bearings, magnetic control of molten iron ore in steel industry, magneto-hydrodynamic electrical power generation, etc.

---

* To whom correspondence should be addressed

In view of these applications, many researchers (Chakrabarti and Gupta [1], Andersson *et al*. [2], Vajravelu and Nayfeh [3], Cortell [4], Ishak *et al*. [5], Chien-Hsin [6], Prasad *et al*. [7], Elbashbeshy and Aldawody [8], Sweet *et al*. [9], Abbasbandy *et al*. [10] and Prasad *et al*. [11]) have analyzed these problems by considering magnetic field with different geometry and physical situation, but in recent years, the study of the diffusion of spices with chemical reaction in the boundary layer flow has gained momentum because of its universal occurrence in many branches of science and engineering. These applications include water and air pollutions, fibrous insulation, atmospheric flows and many other chemical engineering problems. Considering these applications, Chambre and Young [12] examined the development of a first-order reaction in the neighborhood of a flat plate by considering two types of chemical reaction. In one of the cases the reactant is destroyed; in the other, it is generated. Das *et al*. [13] examined the effect of mass transfer on flow over an impulsively started infinite vertical plate in the presence of constant heat flux and chemical reaction. Further, Prasad *et al*. [14] concentrated on a porous medium, obtained numerical solutions and analyzed the diffusion of chemically reactive species of a non-Newtonian fluid immersed in a porous medium over a stretching sheet, and brought out several motivating aspects of the problem. Akyildiz *et al*. [15] observed the flow and mass transfer of a chemically reactive species of a non-Newtonian fluid immersed in a porous medium over a stretching sheet, using the proper sign for the material constant $\alpha \geq 0$ and obtained the concentration c of the reactive species as a solution to a nonlinear boundary value problem over the infinite domain $(0, +\infty)$. Chamkha *et al*. [16] presented an analysis to investigate the effects of chemical reaction on unsteady free convective heat and mass transfer on a stretching surface in a porous medium. Vajravelu *et al*. [17] extended the work of Akyildiz *et al*. [15] to non-Newtonian UCM fluid over a permeable surface by taking the magnetic effect into account. Recently, Mabood *et al*. [18] obtained the chemical reaction effects on MHD stagnation point flow and heat transfer toward a stretching surface with suction/injection using homotopy analysis method (HAM).

All the above investigators restricted their analyses to two dimensional fluid flow over a flat plate/vertical plate. Flow over cylinders is considered to be two-dimensional when the radius of the cylinder is large compared to the boundary layer thickness. For a thin cylinder the radius of the cylinder may be of the same order as that of the boundary layer thickness. Therefore, the flow may be considered as axisymmetric instead of two-dimensional. In this case, the governing equations contain the transverse curvature effect. This may have a strong influence on the velocity, temperature, and the species diffusion fields. The effect of transverse curvature is important in certain applications such as wire or fiber drawing, where accurate prediction of flow heat and mass transfer characteristics is required and a thick boundary layer can exist on slender or near slender bodies. In view of this, Lin and Shih [19; 20] analyzed the laminar boundary layer and heat transfer along cylinders moving horizontally and vertically with constant velocity and established that due to the curvature effect of the cylinder similarity solutions could not be obtained. Ganesan and Loganathan [21] analyzed the effects of heat and mass transfer on the natural convection flow of an incompressible viscous fluid past a semi-infinite isothermal vertical cylinder. Further, Bachok and Ishak [22; 23] investigated the steady mixed convection flow along a permeable vertical/horizontal cylinder with prescribed surface heat flux. Recently, Vajravelu *et al*. [24] studied the effects of transverse curvature and the temperature dependent thermal conductivity on the MHD axisymmetric flow and heat transfer characteristics of a viscous incompressible fluid induced by a non-isothermal stretching cylinder in the presence of internal heat generation/ absorption. Very recently, Hayat *et al*. [25] considered the effects of variable thermal conductivity and variable surface temperature and analyzed the flow of a viscoelastic fluid due to an impermeable stretching cylinder using the homotopy analysis method (HAM).

The available literature on the convective flow, heat and mass transfer with chemical reaction over a stretching sheet/cylinder reveals that not much work has been carried out for convective flow heat and mass transfer over a vertical slender cylinder. Buoyancy is one of the important phenomena in an environment where the difference between land and air temperatures can give rise to complicated flow patterns Therefore; the authors study the combined effects of buoyancy and the homogeneous first order chemical reaction on the axisymmetric flow over a vertical slender cylinder in the presence of transverse magnetic field. In the present analysis, we have considered MHD heat and mass transfer mixed convective axisymmetric flow over a slender cylinder with chemically reactive species (in contrast to the work of Bachok and Ishak [23]). The transformed systems of equations with the appropriate boundary conditions are solved numerically by a second order finite difference scheme for different values of the physical parameters. The effects of the physical parameters on the velocity, temperature, concentration fields are presented graphically and the local skin friction coefficient, the local Nusselt number and the Sherwood number are presented in Tables.

2. Mathematical formulation

Consider a steady, two-dimensional convective flow of a viscous, incompressible fluid, with a chemical reaction, past an impermeable vertical slender cylinder of constant radius *R*. Also, a uniform magnetic field of strength B_0 is applied in the positive *y*-direction, which produces magnetic effect in the *x*-direction. The magnetic Reynolds number is assumed to be small and also assumed that there is no applied electric field and the Hall effect is neglected. The physical model and coordinate system of the problem are shown in Fig.1.

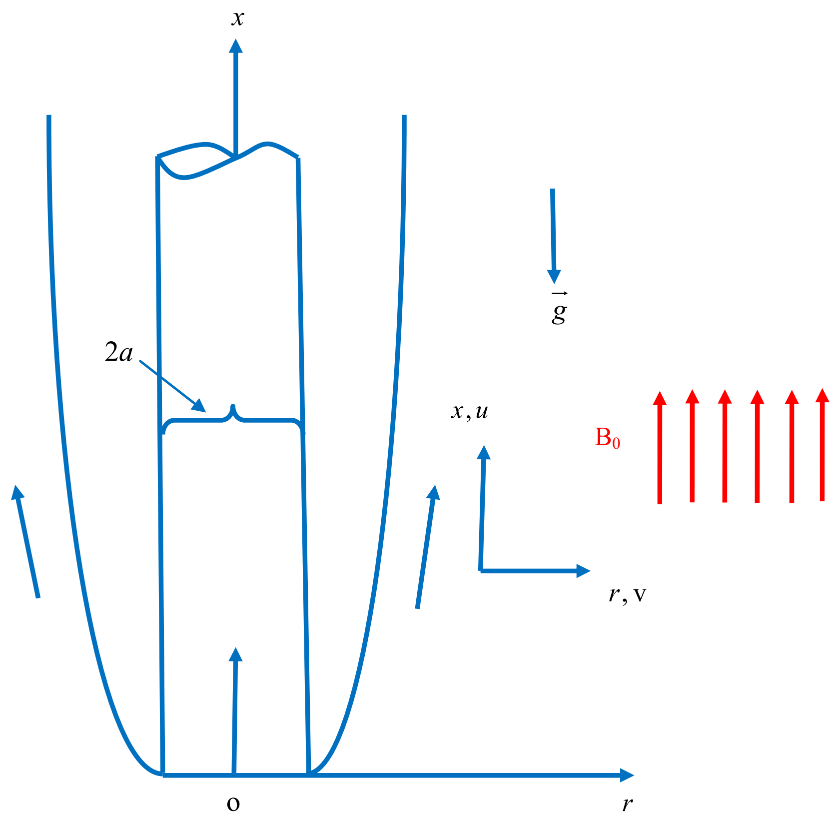

Fig.1. Physical model and coordinate system.

Here, the radial coordinate *r* is measured from the axis of the cylinder and the axial coordinate *x* is measured upwards such that $x=0$ corresponds to the leading edge, where the boundary layer thickness is zero. The radius of the slender cylinder is the same as the order of the boundary layer thickness and hence the flow is taken to be axisymmetric. The cylinder is stretched linearly along the axial coordinate, keeping the origin fixed. The vertical slender cylinder is assumed to have the linear stretching velocity $U_w(x)$, the prescribed surface temperature $T_w(x)$ and the prescribed species diffusion $C_w(x)$, which are of the form $U_w(x)=a(x/l)$, $T_w(x)=T_\infty+b(x/l)$, and $C_w(x)=C_\infty+c(x/l)$, respectively. Here, a is the stretching rate, l is the reference length; b and c are constants whose values depend on the properties of the fluid. The fluid at the edge of the boundary layer is maintained at a constant temperature T_∞ and the surface of the cylinder has a uniform temperature T_w (T_w or $< T_\infty$, i.e., the cylinder is either heated or cooled). An appropriate mass transfer analog to the problem would be the flow along a slender cylinder that contains species *A* that is slightly soluble in fluid *B*. Let C_w be the concentration at the surface of the cylinder and the solubility of *A* and *B* and the concentration of *A* far away from the cylinder is C_∞. Also, let the reaction of species *A* with *B* be a first-order homogeneous chemical reaction of rate constant k_1. It is assumed that the concentration of the dissolved *A* is small enough and the physical properties are virtually constant throughout the fluid. The viscous dissipation effects and the pressure gradient term along the boundary layer are negligible in the energy equation, due to the slow stretching motion of the slender cylinder. All the physical properties are assumed to be constant except for the density in the buoyancy force term which is given by the usual Boussinesq approximation. Further, the level of species concentration is taken to be very low and hence the heat generated during chemical reaction can be neglected. Under these assumptions, the basic boundary layer equations governing the flow, heat and mass transfer in the usual notations are

$$(ru)_x + (rv)_r = 0, \tag{2.1}$$

$$uu_x + vu_r = \nu\left(u_{rr} + r^{-1}u_r\right) + g\beta\left(T - T_\infty\right) + g\beta^*\left(C - C_\infty\right) - \sigma B_0^2(x)u, \tag{2.2}$$

$$\rho c_p\left(uT_x + vT_r\right) = r^{-1}\left(k(T)rT_r\right)_r, \tag{2.3}$$

$$uC_x + v\mathrm{C}_r = r^{-1}\left(D(C)rC_r\right)_r - k_1\left(C - C_\infty\right) \tag{2.4}$$

where u and v are the fluid velocity components measured along the x and y directions of the slender cylinder, respectively. Here, ν is the kinematic viscosity of the fluid, g is the acceleration due to gravity, β is the thermal expansion coefficient, β^* is the concentration expansion coefficient, σ is the electric conductivity, B_0 is the uniform magnetic field, ρ is the density of the fluid, c_p is the specific heat at constant pressure, T is the fluid temperature, C is the species concentration in the fluid and k_1 is the reaction rate constant of a first-order homogeneous and irreversible reaction. Here, $k(T)$ is the temperature dependent thermal conductivity and $D(C)$ is the chemical molecular diffusion coefficient of the diffusing species in the fluid, which are assumed to vary as linear functions of temperature and concentration, respectively, in the following forms

$$k(T) = k_\infty\left(1 + \varepsilon_1\left(\frac{T - T}{T_w - T_\infty}\right)\right) \quad \text{and} \quad D(C) = D_\infty\left(1 + \varepsilon_2\left(\frac{C - C_\infty}{C_w - C_\infty}\right)\right) \tag{2.5}$$

where ε_1 and ε_2, respectively, are the variable thermal conductivity and the variable mass diffusivity. The subscripts w and ∞, respectively, denote the conditions at the surface of the cylinder and faraway from the cylinder. It is further assumed that the surface of the cylinder is maintained at temperature T_w and concentration C_w. The appropriate boundary conditions for the problem are

$$u = U_w, \quad v = 0, \quad T = T_w, \quad C = C_w \quad \text{at} \quad r = R,$$
$$u \to 0, \quad T \to T_\infty, \quad C \to C_\infty \quad \text{as} \quad r \to \infty. \tag{2.6}$$

The particular forms of U_w, T_w and C_w are chosen to devise a similarity transformation, which transform the governing partial differential Eqs (2.2) - (2.4) into a set of ordinary differential equations. It is convenient to reduce the number of equations from four to three and to transform them to a dimensionless form. This can be done by applying the following transformations (See for details Bachok and Ishak [22])

$$\eta = \frac{r^2 - R^2}{2R}\left(\frac{U_w}{\nu x}\right)^{\frac{1}{2}}, \quad \psi = \left(\nu x U_w\right)^{\frac{1}{2}} R f(\eta), \quad \theta(\eta) = \frac{T - T_\infty}{T_w - T_\infty}, \quad \phi(\eta) = \frac{C - C_\infty}{C_w - C_\infty}. \tag{2.7}$$

In Eq.(2.7), ψ is the stream function defined as $u = r^{-1}\psi_r$ and $v = -r^{-1}\psi_x$, which identically satisfies the continuity Eq.(2.1) By defining η in the above form, the boundary condition at $r = R$ reduces to the boundary condition at $\eta=0$, which is more convenient for analytical/numerical computations. Substituting Eqs (2.5) - (2.7), into Eqs (2.2) - (2.4), we get

$$\left(\left(1 + 2\eta\gamma\right) f''\right)' - \left(f'\right)^2 + ff'' + \mathrm{Gr}\,\theta + \mathrm{Gc}\,\phi - Mnf' = 0, \tag{2.8}$$

$$\left(1 + 2\eta\gamma\right)\left(\left(1 + \varepsilon_1\theta\right)\theta'\right)' + 2\left(1 + \varepsilon_1\theta\right)\gamma\theta' - \mathrm{Pr}\left(f'\theta - f\theta'\right) = 0, \tag{2.9}$$

$$\left(1 + 2\eta\gamma\right)\left(\left(1 + \varepsilon_2\phi\right)\phi\right)' + 2\left(1 + \varepsilon_2\phi\right)\gamma\phi' - \mathrm{Sc}\left(f'\phi - f\phi'\right) - \delta\mathrm{Sc}\phi = 0 \tag{2.10}$$

where a prime denotes differentiation with respect to η. The corresponding boundary conditions (2.6) become

$$f' = 1, \quad f = 0, \quad \theta = 1, \quad \phi = 1 \quad \text{at} \quad \eta = 0,$$
$$f' = 0, \quad \theta = 0, \quad \phi = 0 \quad \text{as} \quad \eta \to 0. \tag{2.11}$$

The parameters γ, Gr, Gc, Mn Pr, Sc and δ are the transverse curvature, the thermal Grashof number, the mass Grashof number, the magnetic parameter, the Prandtl number, the Schmidt number and the reaction rate parameter, respectively, and are defined as

$$\gamma = \sqrt{\frac{l\nu}{aR^2}}, \quad \mathrm{Gr} = \frac{g\beta b l^{5/2}\nu^{1/2}}{ka^{5/2}}, \quad \mathrm{Gc} = \frac{g\beta^* d\, l}{a^2}, \quad Mn = \frac{\sigma B_0^2 l}{\rho b},$$
$$\mathrm{Pr} = \frac{\mu c_p}{k_\infty}, \quad \mathrm{Sc} = \frac{\nu}{D_\infty} \quad \text{and} \quad \delta = \frac{k_1 l}{a}. \tag{2.12}$$

From the mass diffusion Eq.(2.10), we can see the following three cases:

(i) $\delta > 0$, implies the destructive chemical reaction;

(ii) $\delta = 0$, implies no chemical reaction; and
(iii) $\delta < 0$, implies the generative chemical reaction.

The physical quantities of interest are the skin friction coefficient C_f, the local Nusselt number Nu_x and the local Sherwood number Sh_x which are defined by

$$C_f = \frac{\tau_w}{\rho U_w^2/2}, \quad \mathrm{Nu}_x = \frac{x q_w}{k_\infty (T_w - T_\infty)}, \quad \mathrm{Sh}_x = \frac{x q_m}{D_\infty (C_w - C_\infty)} \tag{2.13}$$

where the surface shear stress, the surface heat flux and the surface mass flux are given by

$$\tau_w = \mu \left(\frac{\partial u}{\partial r} \right)_{r=a}, \quad q_w = -k_\infty \left(\frac{\partial T}{\partial r} \right)_{r=a}, \quad q_m = -D_\infty \left(\frac{\partial C}{\partial r} \right)_{r=a}, \tag{2.14}$$

with μ being the viscosity and k_∞ is the thermal conductivity, respectively. Using the similarity variables (2.7), we obtain

$$\frac{1}{2} C_f \,\mathrm{Re}_x^{1/2} = f''(0), \quad \mathrm{Nu}_x \mathrm{Re}_x^{-1/2} = -\theta'(0) \quad \text{and} \quad \mathrm{Sh}_x \mathrm{Re}_x^{-1/2} = -\phi'(0) \tag{2.15}$$

where $\mathrm{Re}_x = U_w x/\nu$ is the local Reynolds number.

3. Exact solutions for some special cases

Here, we present the exact solutions in certain special cases: Such solutions are useful and serve as baseline results for comparison with the solutions obtained via the numerical scheme. For Gr=0 and $\mathrm{Gc}=0$, $Mn = 0$, Eqs (2.8) and (2.9) reduces to the flow considered by Rekha and Naseem [26]. While, in the presence of transverse curvature and $\delta = \mathrm{Gr}=\mathrm{Gc} = \varepsilon_1 = \varepsilon_2 = Mn = 0.0$, Eqs (2.8) - (2.10) reduce to those of Bachok and Ishak [23] , where the closed-form solution is given by

$$f = \frac{1 - e^{-m\eta}}{m}, \quad (m > 0) \quad \text{where} \quad m = \sqrt{1 + Mn}\,. \tag{3.1}$$

Perturbation analysis for heat and mass transfer in the absence of transverse curvature parameter

The solution to the heat and mass transfer Eqs (2.9) and (2.10) can be analyzed in terms of the perturbation analysis

$$\theta(\eta) = \theta_0(\eta) + \varepsilon_1 \theta_1(\eta) + \varepsilon_1{}^2 \theta_2(\eta) + \ldots\ldots\ldots\ldots, \tag{3.2}$$

$$\phi(\eta) = \phi_0(\eta) + \varepsilon_2 \phi_1(\eta) + \varepsilon_2{}^2 \phi_2(\eta) + \ldots\ldots\ldots\ldots \tag{3.3}$$

Substituting this into Eqs (2.9) and (2.10) and equating like powers of ε_1 and ε_2 ignoring quadratic and higher order terms in ε_1 and ε_2, we obtain

$$\theta_0'' + \Pr f\theta_0' - \Pr f'\theta_0 = 0, \tag{3.4}$$

$$\phi_0'' + \mathrm{Sc} f\phi_0' - \mathrm{Sc}\left(f' - \delta\right)\phi_0 = 0, \tag{3.5}$$

with boundary conditions

$$\theta_0(0) = 1, \quad \phi_0(0) = 1, \quad \theta_0(\infty) = 0, \quad \phi_0(\infty) = 0. \tag{3.6}$$

Also

$$\theta_1'' + \Pr f\theta_1' - \Pr f'\theta_1 = -\theta_0\theta_0'' - \theta_0'^2, \tag{3.7}$$

$$\phi_1'' + \mathrm{Sc} f\phi_1' - \mathrm{Sc}\left(f' - \delta\right)\phi_1 = -\phi_0\phi_0'' - \phi_0'^2, \tag{3.8}$$

with the boundary conditions

$$\theta_1(0) = 0, \quad \theta_1(\infty) = 0, \quad \phi_1(0) = 0, \quad \phi_1(\infty) = 0. \tag{3.9}$$

Equations for θ_0 and ϕ_0 can be solved explicitly in terms of confluent hypergeometric series, namely Kummer's function $\mathrm{M}(a,b,z)$ (see for details Abramowitz and Stegun [27]) and are given by

$$\theta_0(\eta) = C_4 \exp\left(-\Pr m\,\eta\right)\mathrm{M}\left(a_1, b_1, z\right), \qquad z = -\Pr/m^2 \exp\left(-m\eta\right),$$

$$\frac{1}{C_4} = \mathrm{M}\left(a_1, b_1, -\Pr\right), \qquad a_1 = \left(\Pr - 1\right), \qquad b_1 = 1 + \Pr, \tag{3.10}$$

$$\phi_0(\eta) = \exp\left(-\frac{\left(a_0 + b_0\right)m\eta}{2}\right)\mathrm{M}\left(a_{11}, b_{11}, -\mathrm{Sc}\,e^{-m\eta}\right)\Big/\mathrm{M}\left(a_{11}, b_{11}, -\mathrm{Sc}\right)$$

where $\quad a_0 = \mathrm{Sc}, \quad b_0 = \sqrt{\mathrm{Sc}^2 + 4\delta\mathrm{Sc}}, \qquad a_{11} = \dfrac{a_0 + b_0 - 2}{2}, \quad b_{11} = 1 + b_0.$

4. Numerical procedure

Equations (2.8) - (2.10) are highly non-linear and coupled ordinary differential equations with variable coefficients. Exact analytical solutions are not possible for the complete set of Eqs (2.8) - (2.10). Hence, we use the efficient numerical method with second order finite difference scheme known as the Keller-box method. The boundary value problem (2.8) - (2.10) is reduced to a system of seven simultaneous ordinary differential equations of first order for seven unknowns following the method of superposition. To solve the system of first order equations we require seven initial conditions whilst we have only two initial conditions on f and one initial condition of each of θ and ϕ. The three initial conditions $f''(0)$, $\theta'(0)$ and $\phi'(0)$ are not known. However, the values of $f'(\eta)$, $\theta(\eta)$ and $\phi(\eta)$ are known as $\eta \to \infty$. Now, we employ the Keller-box scheme where these three boundary conditions are utilized to produce three unknown initial conditions at $\eta = 0$. To select η_∞, we begin with some initial guess value of the unknown initial conditions and solve the boundary value problem to obtain $f''(0)$, $\theta'(0)$ and $\phi'(0)$. Let α_0, β_0 and γ_0 be the correct values of $f_3(0), \theta_2(0)$ and $\phi_2(0)$, respectively and integrate the system using the fourth order Runge-Kutta method and denote the values of $f_3(0), \theta_2(0)$ and $\phi_2(0)$, respectively. The solution process is repeated with another larger value of η_∞ until two successive values of unknown conditions differ only according to the desired accuracy. The last value of η_∞ is chosen as an appropriate value for that particular set of parameters. Then solve the system of equations by the Keller-box method (See for details Cebeci and Bradshaw, [28]; Keller [29]; Vajravelu and Prasad [30]). The numerical solutions are obtained in the following four steps:

- reduce Eqs (2.8) - (2.10) to a system of first-order equations;
- write the difference equations using central differences;
- linearize the algebraic equations by Newton's method, and write them in a matrix-vector form; and
- solve the linear system by the block tri-diagonal elimination technique.

For numerical calculations, a uniform step size of $\Delta\eta = 0.01$ is found to be satisfactory and the shooting error was controlled with an error tolerance of 10^{-6} in all the cases. The physical domain in this problem is unbounded, whereas the computational domain has to be finite and due to this reason, we apply the far field boundary conditions for the similarity variable η at a finite value denoted by $\eta_{\max}$. A value of $\eta_{\max} = 12$ is found to be sufficient to achieve the far field boundary conditions asymptotically for all values of the parameters considered. To assess the accuracy of the present method, a comparison of the skin friction and the wall-temperature gradient between the present results and the previously published results is presented, for special cases, our results are found to be in good agreement with those of the results available in the literature, which is shown in Tabs 1, 2 and 3. It is obvious from the Tab.3 that the relative percentage error occurred in the heat transfer rate $\theta'(0)$ of the above mentioned references is due to the similar transformation used in their papers for Newtonian fluid case.

Table 1. Comparison of $-f''(0)$ for $\gamma = \mathrm{Gc} = \mathrm{Gr} = 0.0$, $\mathrm{Pr} = 1.0$.

$-f''(0)$				
Mn	Exact solution	Andersson *et al.* [2] for $n = 1$	Vajravelu *et al.* [24]	Present values
0.0	*1.000000*	*1.00000*	*1.000001*	*1.00000*
0.5	*1.224745*	*1.2249*	*1.224745*	*1.224745*
1.0	*1.414214*	*1.4140*	*1.414214*	*1.414214*
1.5	*1.581139*	*1.58100*	*1.581139*	*1.581139*
2.0	*1.732051*	*1.73200*	*1.732051*	*1.732051*

Table 2. Comparison of $-f''(0)$ for $Gr = 1.0$ when $Pr = 1.0$, $Gc = Sc = \gamma = \varepsilon_1 = \varepsilon_2 = \delta = Mn = 0.0$.

Ishak *et al.* [5]	Chien-Hsin [6]	Elbashbeshy and Aldawody [8]	Present results
0.5607	*0.5607*	*0.5608*	*0.5607567*

Table 3. Comparison of the values of $-\theta'(0)$ for different values of Pr when $Gr = Gc = Sc = \gamma = = \varepsilon_1 = \varepsilon_2 = \delta = 0.0$.

	Mn = 0.0							*Mn* = 1.0		
Pr	Present results	Grubkha and Bobba [31]	Ali [32]	Ishak *et al*. [33]	Relative error Grubkha and Bobba [31]	Relative error Ali [32]	Relative error Ishak *et al.* [33]	Present results	Prasad *et al*. [7] for linear stretching	Relative error Prasad *et al.* [7]
0.72	*0.808631*	*0.8086*	*0.8058*	*0.808631*	*0.00383364*	*0.350097881*	*0.0*	*0.5054647*	*0.50546*	*0.000929837*
1.0	*1.0*	*1.0*	*0.9961*	*1.0*	*0.0*	*0.390000000*	*0.0*	*0.5054647*	*0.50546*	*0.000929837*
3.0	*1.923663*	*1.9237*	*1.9144*	*1.923682*	*0.001923414*	*0.481529249*	*0.0009877*	*1.075216*	*1.07522*	*0. 000372018*
10.0	*3.720649*	*3.7207*	*3.7006*	*3.720673*	*0.001370729*	*0.538857603*	*0.00064505*	*2.217622*	**	**

Table 4. Numerical values of the skin friction, wall temperature gradient and mass concentration gradient for different values of the pertinent parameters.

Sc	Pr	δ	ε_1	ε_2	Gr	Gc	Mn	$\gamma=0.0$			$\gamma=0.5$			$\gamma=1.0$		
								$-f''(0)$	$-\theta'(0)$	$-\phi'(0)$	$-f''(0)$	$-\theta'(0)$	$-\phi'(0)$	$-f''(0)$	$-\theta'(0)$	$-\phi'(0)$
0.96	1.0	0.1	0.1	0.1	0.5	0.5	0.0	0.55301	1.01796	1.04104	0.69858	1.20427	1.23172	0.85335	1.37424	1.40410
							0.5	0.78946	0.97312	1.00083	0.95913	1.15341	1.18656	1.12741	1.32441	1.35942
							1.0	0.99460	0.93415	0.96644	1.17940	1.11114	1.14949	1.35810	1.28338	1.32291
						0.0	0.5	0.76371	0.98305	1.00948	0.92163	1.16609	1.19793	1.08299	1.33384	1.36844
						0.5		0.55300	1.01797	1.04104	0.69476	1.20481	1.23247	0.84252	1.37412	1.40451
						1.0		0.35433	1.04661	1.06724	0.48249	1.23610	1.26077	0.61809	1.40702	1.43428
					-	0.5		0.85840	0.96384	0.99242	1.02756	1.14317	1.17790	1.19521	1.31096	1.34824
					0.0			0.76697	0.98181	1.00840	0.92704	1.16394	1.19609	1.08888	1.33182	1.36668
					1.0			0.35275	1.04703	1.06763	0.47978	1.23691	1.26148	0.61486	1.40790	1.43507
				0.0	0.5			0.55789	1.01667	1.11229	0.70034	1.20336	1.31173	0.84865	1.37262	1.49129
				0.2				0.54837	1.01923	0.98065	0.68945	1.20623	1.16541	0.83671	1.37557	1.33118
				0.4				0.53979	1.02166	0.88342	0.67958	1.20895	1.05777	0.82589	1.37836	1.21369
			0.0	0.1				0.55798	1.08796	1.03984	0.70049	1.28258	1.23112	0.84880	1.45926	1.40312
			0.2					0.54829	0.95863	1.04222	0.68930	1.13902	1.23378	0.83656	1.30219	1.40586
			0.4					0.53953	0.86308	1.04448	0.67916	1.03339	1.23631	0.82548	1.18693	1.40844
		-0.5	0.1					0.50234	1.03572	0.70000	0.62658	1.22804	0.84436	0.77679	1.39392	100806
		0.0						0.54779	1.01967	0.99528	0.68793	1.20706	1.18281	0.83520	1.37628	1.35230
		0.5						0.56916	1.01291	1.20342	0.71507	1.19838	1.40484	0.86491	1.36764	1.58542
	0.71	0.1						0.52741	0.84399	1.04907	0.66873	1.03254	1.24006	0.81771	1.20357	1.41101
	1.0							0.55300	1.01797	1.04104	0.69475	1.20481	1.23247	0.84252	1.37412	1.40451
	2.0							0.60097	1.50035	1.02788	0.74819	1.68645	1.21802	0.89761	1.85683	1.39072
	5.0							0.65113	2.46633	1.01767	0.80490	2.65052	1.20616	0.96023	2.82679	1.37770
	7.0							0.66614	2.94408	1.01537	0.82143	3.13166	1.20357	0.97836	3.30984	1.37479
0.22	1.0							0.43971	1.05888	0.45383	0.58809	1.24069	0.65248	0.73931	1.40411	0.83327
0.71								0.53046	1.02577	0.87859	0.67162	1.21239	1.07091	0.82002	1.38071	1.24361
1.0								0.55595	1.01698	1.06510	0.69788	1.20381	1.25645	0.84565	1.37321	1.42849
2.0								0.60189	1.00328	1.56193	0.74863	1.18869	1.75289	0.89876	1.35853	1.92747
5.0								0.65043	0.99266	2.55366	0.80269	1.17649	2.74519	0.95817	1.34517	2.92545

5. Results and discussion

Employing the above numerical method, the governing equations of the problem are solved for several sets of values of pertinent parameters, namely, the transverse curvature parameter γ, the thermal Grashof number Gr, the mass Grashof number Gc, the magnetic parameter *Mn*, the variable thermal conductivity parameter ε_1, the Prandtl number Pr, the variable mass diffusivity parameter ε_2, the Schmidt number Sc and the reaction rate parameter δ. In order to analyze the salient features of the problem, the numerical results are presented graphically in Figs 2-6. Also the numerical results for the skin friction coefficient, the Nusselt number and the Sherwood number are presented in Tab.4.

Figures 2a through 2c elucidate the effect of increasing values of γ and *Mn* on $f'(\eta), \theta(\eta)$ and $\phi(\eta)$. It is clear from all the three profiles that there is an increase in the magnitude of velocity, temperature and concentration boundary layer thickness for increasing values of γ. That is, the boundary layer thickness is higher for non-zero values as compared to the zero value of γ. Figure 2a shows that $f'(\eta)$ decreases for increasing values of *Mn* and this is because of the induction of the transverse magnetic field (normal to the flow direction) which has a tendency to induce a drag, known as the Lorentz force, which tends to resist the flow whereas in the case of $\theta(\eta)$ and $\phi(\eta)$ the effect of *Mn* is quite opposite (See Fig.2b and Fig.2c). A similar trend can be observed for the skin friction, wall temperature gradient and mass concentration gradient for increasing values of *Mn* (See Tab.4 for details).

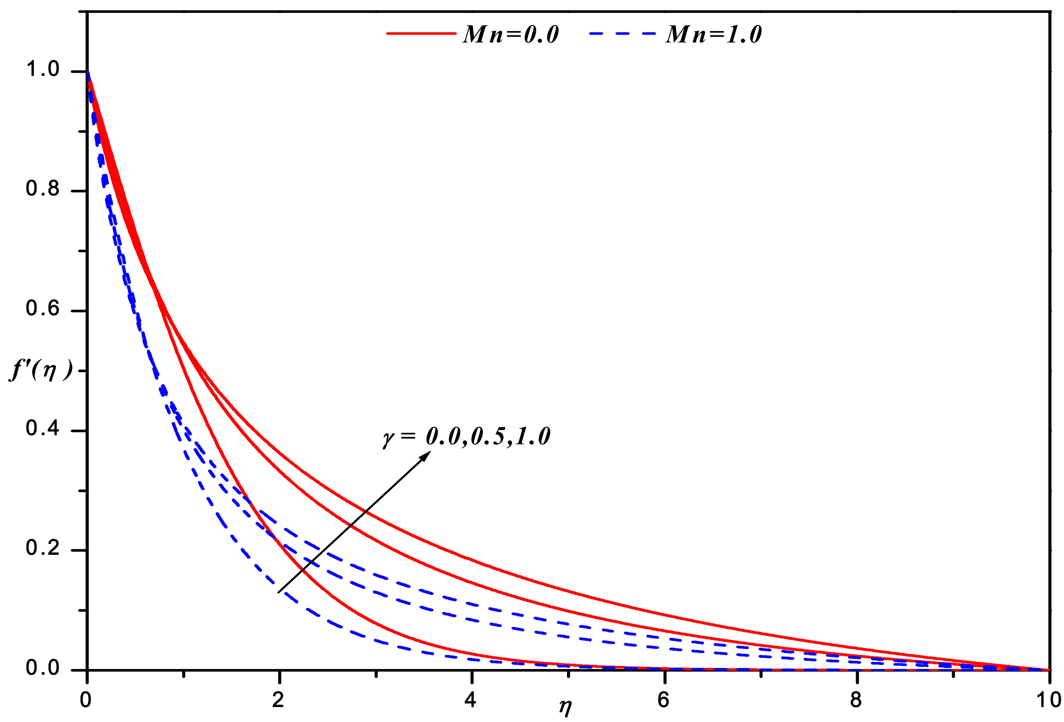

Fig.2a. Velocity profiles for different values of γ with Pr=*1.0*, Sc=*0.96*, Gr=*0.5*, Gc=*0.5*, $\varepsilon_1 = 0.1$, $\varepsilon_2 = 0.1$ and $\delta = 0.1$.

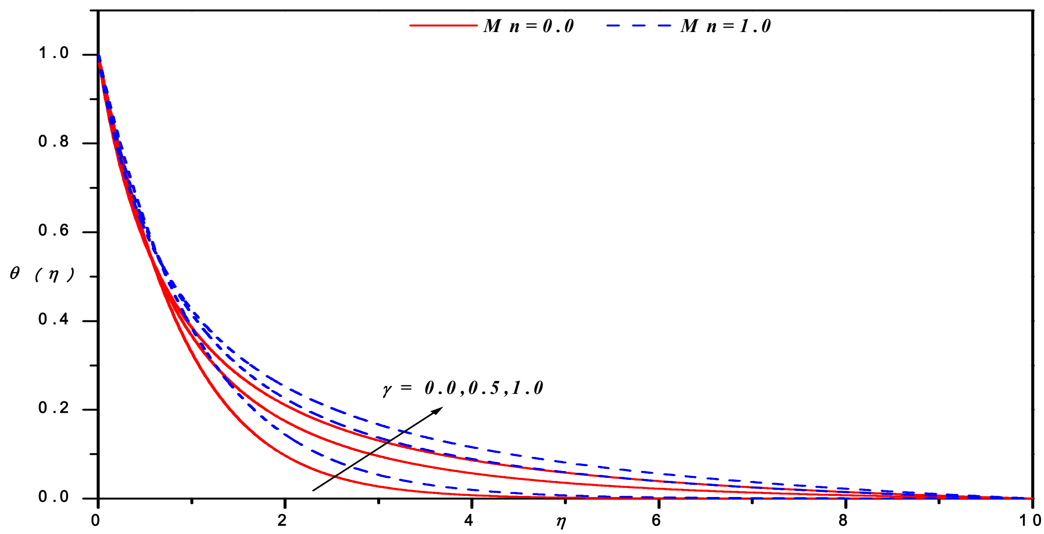

Fig.2b. Temperature profiles for different values of γ and *Mn* with Pr=*1.0*, Sc=*0.96*, Gr=*0.5*, Gc=*0.5*, $\varepsilon_1 = 0.1$, $\varepsilon_2 = 0.1$ and $\delta = 0.1$.

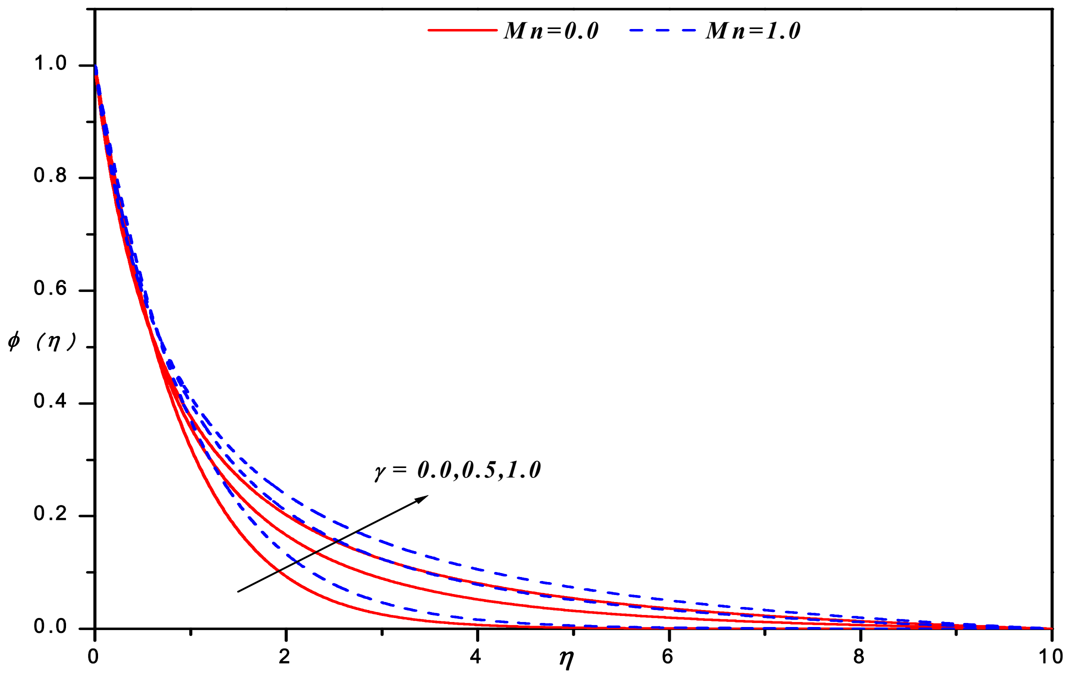

Fig.2c. Concentration profiles for different values of γ and *Mn* with Pr=*1.0*, Sc=*0.96*, Gr=*0.5*, Gc=*0.5*, $\varepsilon_1 = 0.1$, $\varepsilon_2 = 0.1$ and $\delta = 0.1$.

Figures 3a and 3b are the graphical representation of the axial velocity $f'(\eta)$ for different values of Gr and Gc. From these figures, it is observed that the axial velocity profile decreases monotonically and tends asymptotically to zero as the distance increases from the slit. These figure demonstrates that an increase in Gr leads to an increase in the axial velocity in the absence of species diffusion. This phenomenon is even true in the presence of species diffusion. Further, an increase in Gr means an increase in the temperature gradient leading to the enhancement of the axial velocity, due to enhanced convection.

Physically, Gr<*0* corresponds to an externally heated plate because the free convection currents are carried towards to the plate, Gr>*0* corresponds to an externally cooled plate and Gr=*0* corresponds to the absence of free convection currents. A comparison of the curves in Fig.3a reveals that the introduction of chemical species diffusion leads to an increase in the axial velocity in both cases of heating and cooling of the fluid. This is due to the fact that Gc depends upon $C_w - C_\infty$ and here we assume it to be positive. That is, the level of concentration is higher near the plate than that away from the surface. This observation is even true for non-zero values of the curvature parameter shown graphically in Fig.3b. The effects of buoyancy parameters namely, Gr and Gc on the temperature profiles for zero and non-zero values of γ are shown graphically in Figs 4a and 4b, respectively. The general trend is that the temperature distribution is unity at the surface; but with changes in the physical parameters the temperature decreases with the distance from the slender cylinder. It is observed that the effect of increasing values of Gr results in a decrease in the thermal boundary layer thickness; this is associated with an increase in the magnitude of the wall temperature gradient and hence results in an increase in the surface heat transfer. This is true even with Gc. Effects of species diffusion and the curvature parameter are shown graphically in Fig.4b. A comparison with Fig.4a reveals that the presence of γ is to increase the temperature and hence to enhance the thermal boundary layer thickness. The dimensionless concentration profiles are presented in Fig.5. The behaviors of the buoyancy parameters, namely, Gr and Gc are depicted graphically in Fig.5a. It is noticed that the effect of Gr is to decrease the concentration distribution; as the concentration species dispersed away are largely due to the temperature gradient. A comparison of the curves reveals that the effect of Gc is to decrease the concentration profile significantly in the case of cooling of the fluid. This is because of the fact that the concentration gradient accelerates the dispersion of the species. Figure 5b demonstrate the effect of Sc and ε_2 on $\phi(\eta)$. The effect of Sc is to decrease the concentration distribution in the boundary layer. This is due to the thinning of the concentration boundary layer with the introduction of chemical species diffusion. This holds true even in the presence of ε_2. The effect of ε_2 is to increase the species profile which in turn increases the concentration boundary layer thickness. The concentration profile $\phi(\eta)$ across the flow field is plotted in Fig.5c for different values of the reaction rate parameter δ and Gc. From this figure we observe that the effect of increasing the value of δ is to decrease the concentration in the flow field. However, the values for the mass concentration are higher for negative values of δ as compared to positive values of δ. Physically, $\delta < 0$ represents a generative chemical reaction, i.e., the species which diffuses from the stretching surface is produced by a chemical reaction in the free stream; and $\delta > 0$ a destructive chemical reaction, i.e., one that reduces the thickness of the concentration layer and increases the wall transfer, as shown in the figure. The combined effect of buoyancy parameters is to reduce the temperature profile significantly in the flow field. The effects of Pr and ε_1 on the temperature distribution are depicted graphically in Fig.6. We notice that an increase in Pr is to decrease the temperature distribution. This is due to the fact that the presence of temperature-dependent thermal conductivity results in reducing the magnitude of the transverse velocity by a quantity $\partial K(T)/\partial r$ and this can be seen from the energy Eq.(2.3).

The values of the skin friction, the Nusselt number and the Sherwood number for various values of the physical parameters are recorded in Tab.4. $f''(0)$, $\theta'(0)$ and $\phi'(0)$ are found to decrease with an increase in γ in the absence of buoyancy effects. An increase in buoyancy parameters leads to an increase in the skin friction and a decrease in the Nusselt number as well as the Sherwood number. It is interesting to note that the magnitude of the surface mass transfer increases with Sc and δ for non-zero values of γ. The effect of the variable thermal conductivity parameter is to enhance the rate of heat transfer. But the effect of Pr is to decrease the wall-temperature gradient for zero and non-zero values of the buoyancy parameters.

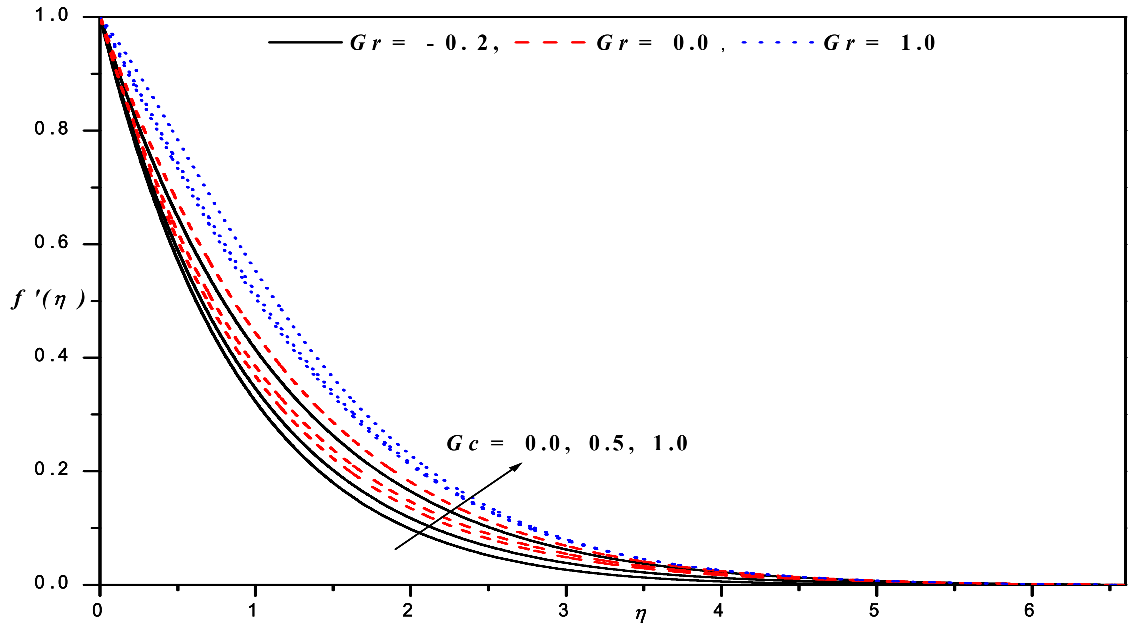

Fig.3a. Velocity profile for different values of Gr and Gc with Pr=*1.0*, *Mn=0.5*, Sc=*0.96*, $\varepsilon_1 = 0.1$, $\varepsilon_2 = 0.1$ and $\delta = 0.1$ when $\gamma = 0.0$.

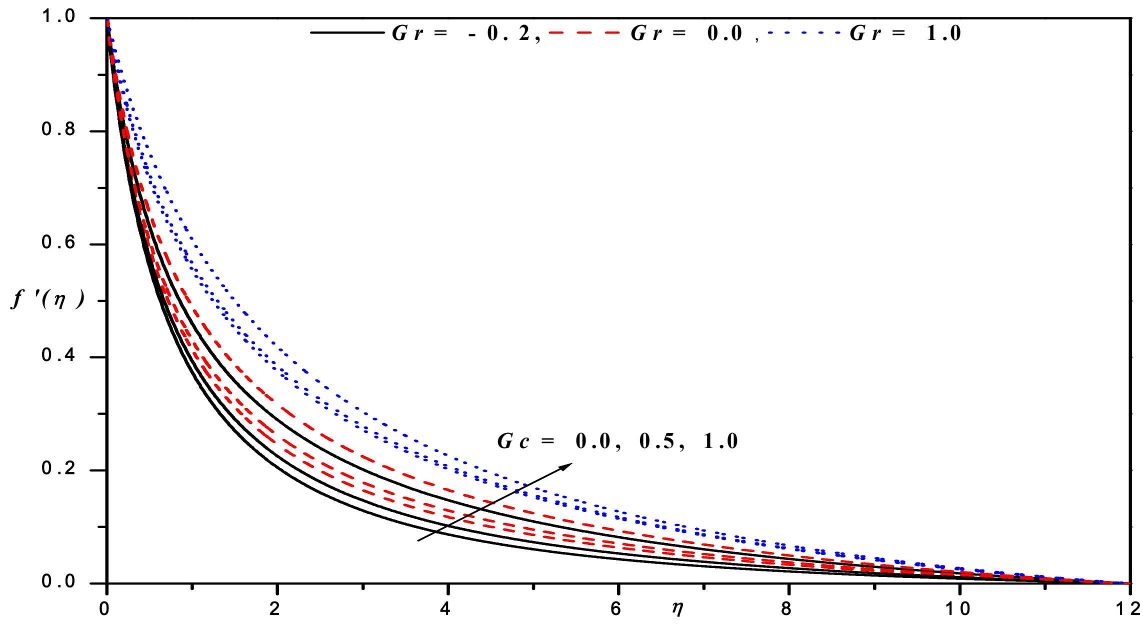

Fig.3b. Velocity profile for different values of Gr and Gc with Pr=*1.0*, *Mn=0.5*, Sc=*0.96*, $\varepsilon_1 = 0.1$, $\varepsilon_2 = 0.1$ and $\delta = 0.1$ when $\gamma = 1.0$.

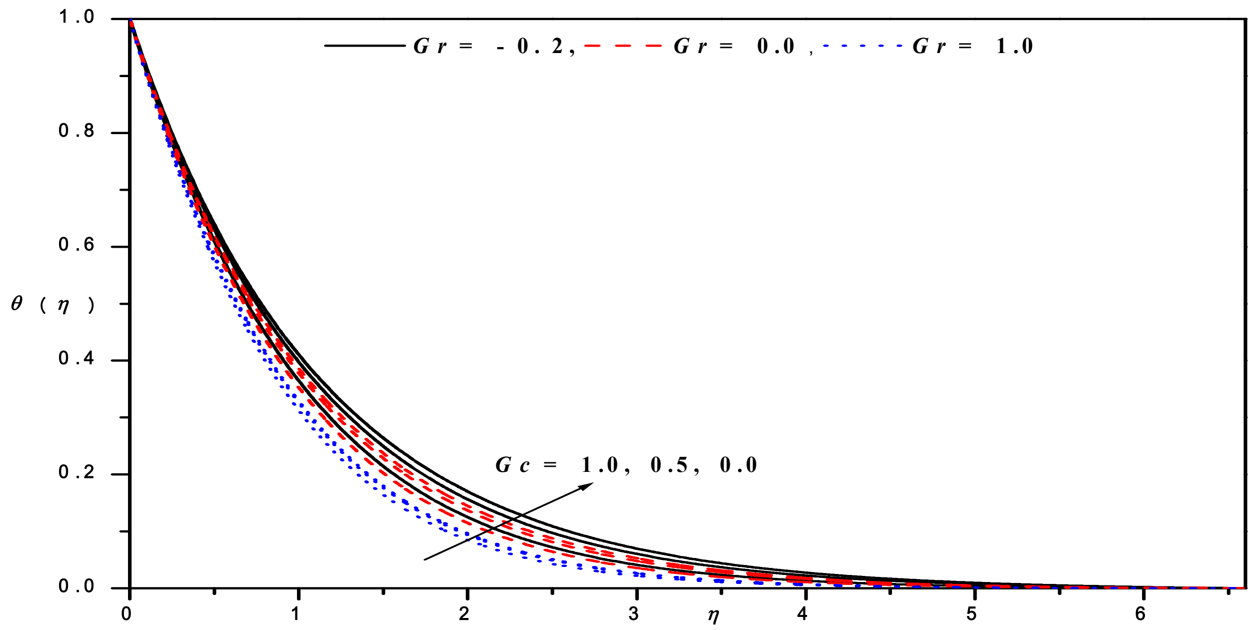

Fig.4a. Temperature profile for different values of Gr and Gc with Pr=*1.0*, *Mn=0.5*, Sc=*0.96*, $\varepsilon_1 = 0.1$, $\varepsilon_2 = 0.1$ and $\delta = 0.1$ when $\gamma = 0.0$.

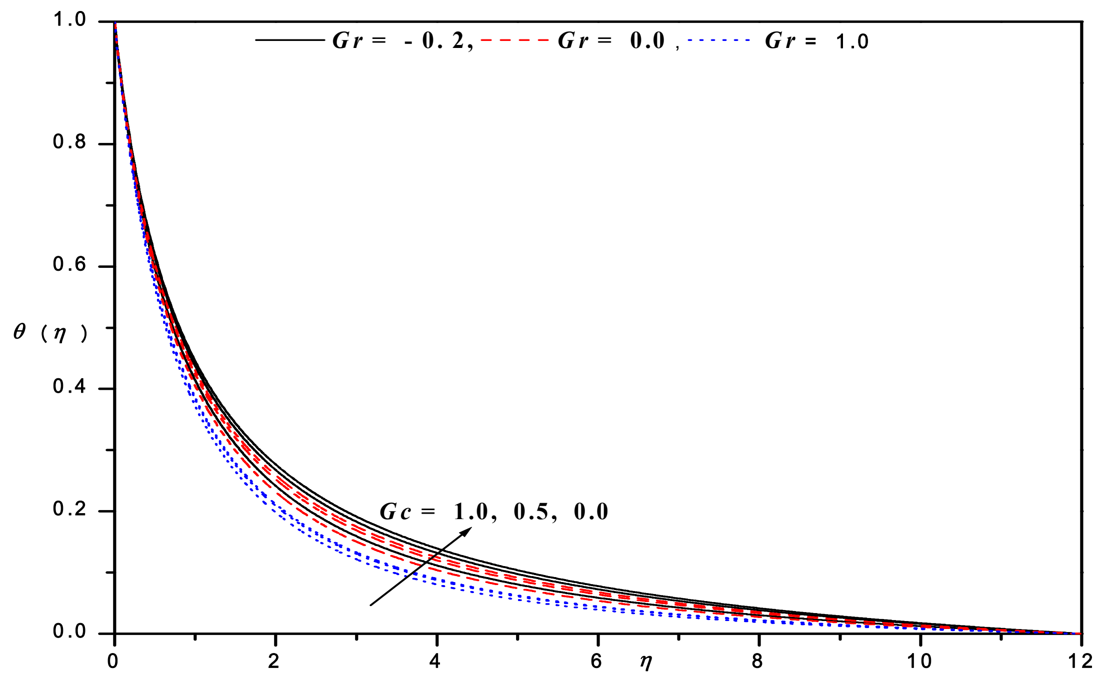

Fig.4b. Temperature profile for different values of Gr and Gc with Pr=*1.0*, *Mn=0.5*, Sc=*0.96*, $\varepsilon_1 = 0.1$, $\varepsilon_2 = 0.1$ and $\delta = 0.1$ when $\gamma = 1.0$.

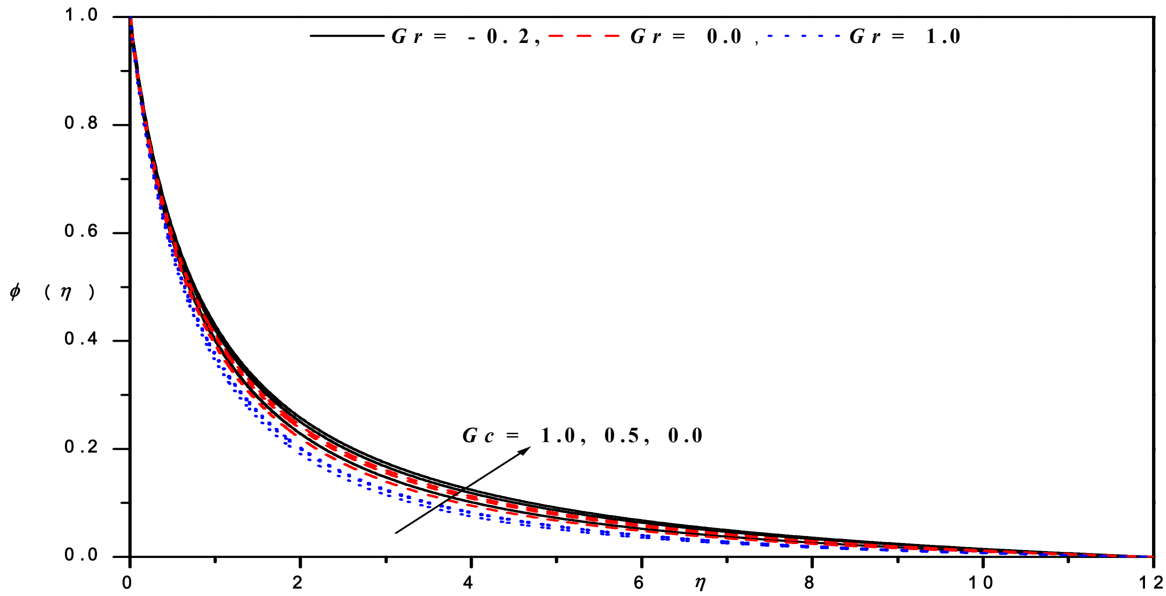

Fig.5a. Concentration profile for different values of Gr and Gc with Pr=1.0, $Mn=0.5$, Sc=0.96, $\varepsilon_1 = 0.1$, $\varepsilon_2 = 0.1$ and $\delta = 0.1$ when $\gamma = 1.0$.

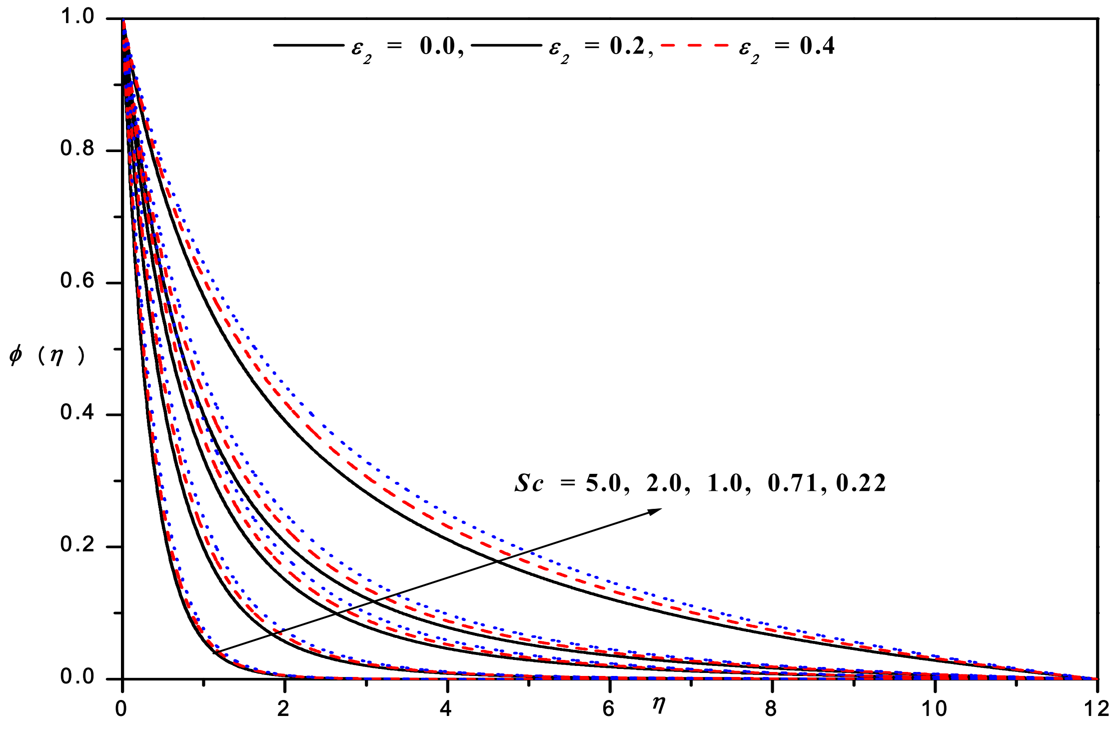

Fig.5b. Concentration profiles for different values of Sc and ε_2 when $Mn=0.5$, $\gamma = 0.5$, Pr=1.0, Gr=0.5, Gc=0.5, $\varepsilon_1 = 0.1$ and $\delta = 0.1$.

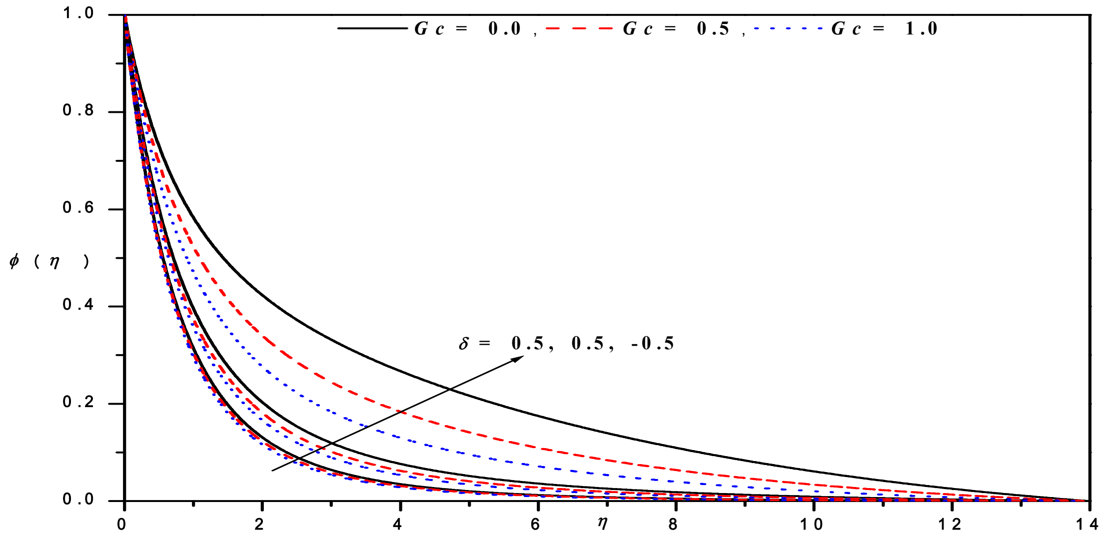

Fig.5c. Concentration profile for different values of δ and Gc with Pr=*1.0*, *Mn=0.5*, , Sc=*0.96*, $\varepsilon_1 = 0.1$, $\varepsilon_2 = 0.1$ and Gc=*0.5* when $\gamma = 0.5$.

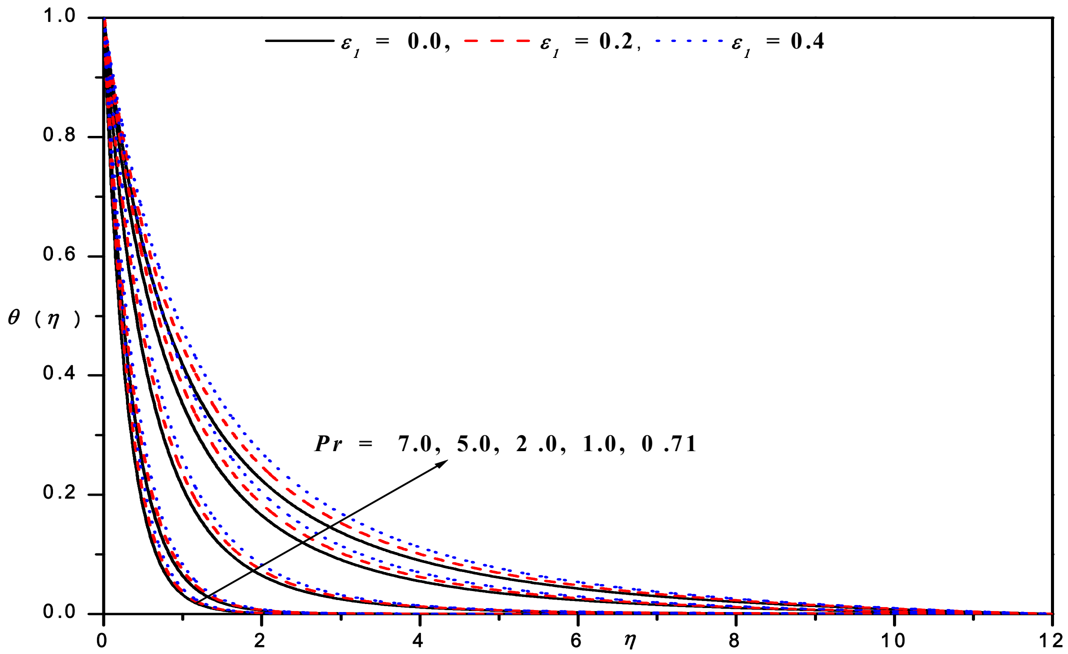

Fig.6. Temperature profile for different values of Pr and ε_1 when *Mn=0.5*, $\gamma = 0.5$, Sc=*0.96*, Gr=*0.5*, Gc=*0.5*, $\varepsilon_2 = 0.1$ and $\delta = 0.1$.

6. Conclusion

The numerical results obtained via the second order finite difference method and their analysis lead to some of the following conclusions:

- The velocity boundary layer thickness increases with an increase in γ, Gr and Gc.
- The effect of increasing values of Gr, Gc and Pr is to decrease the temperature profiles. But the trend is reversed with parameters γ and ε_1.
- An increase in *Mn* leads to a decrease in velocity boundary layer thickness and an increase in thermal as well as concentration boundary layer thickness.
- Concentration profiles decrease with increasing values of Gr, Gc, Sc and δ, but increase with increasing values of γ and ε_2.
- The Nusselt number increases with increasing Mn, γ, ε_1, Sc and δ; but decreases with increasing Gr, Gc, Pr and ε_2.
- The effect of increasing Mn, γ, Pr and ε_2 enhance the Sherwood number and the opposite is true with the parameters Gr, Gc, ε_1, Sc and δ.

Acknowledgments

The authors appreciate the constructive comments of the reviewer which led to definite improvements in the paper. One of the authors (Hanumesh Vaidya) is thankful to the University Grants Commission, New Delhi for financial support under the Minor Research Project (Grant No. MRP(S)-0060/12-13/KAUG062/UGC-SWRO)

Nomenclature

$a, b, a_o, b_0, a_{11}, b_{11}$ – constants
B_0 – uniform magnetic field
C – concentration of the fluid
C_f – skin friction coefficient
C_w – concentration at the surface
C_∞ – concentration of the fluid far away from the wall
c_p – specific heat at constant pressure
$D(C)$ – concentration dependent diffusion coefficient
D_∞ – diffusion coefficient far away from the wall
f – dimensionless stream function
Gc – mass Grashof number
Gr – thermal Grashof number
g – acceleration due to gravity
$k(T)$ – temperature-dependent thermal conductivity
k_w – thermal conductivity at the wall
k_1 – chemical reaction parameter
k_∞ – thermal conductivity far away from the wall
l – reference length scale
M – Kummer's function
Mn – magnetic parameter
Nu_x – local Nusselt number
Pr – Prandtl number
R – radius of the cylinder
Re_x – local Reynolds number

r – radial coordinate
Sc – Schmidt number
Sh_x – local Sherwood number
T – fluid temperature
T_w – surface temperature
T_∞ – ambient temperature
U_w – stretching velocity
u – axial velocity component
v – radial velocity component
x – axial coordinate
β – thermal expansion coefficient
β^* – concentration expansion coefficient
γ – transverse curvature
δ – reaction rate parameter
ε_1 – variable thermal conductivity
ε_2 – variable diffusivity
η – similarity variable
θ – dimensionless temperature
μ – dynamic viscosity
ν – kinematic viscosity
ρ – density
σ – electric conductivity
ϕ – dimensionless concentration
ψ – stream function

Subscript

w – conditions at the stretching sheet
∞ – condition at infinity

Superscript

$'$ – differentiation with respect to η

References

[1] Chakrabarti A. and Gupta A.S. (1979): *Hydromagnetic flow and heat transfer over a stretching sheet.* – Quart. Appl. Math., vol.8, pp.73-78.

[2] Andersson H.I., Bech K.H. and Dandapat B.S. (1992): *Magnetohydrodynamic flow of a power law fluid over a stretching sheet.* – Int. J. Non-Linear Mech., vol.27, pp.929-936.

[3] Vajravelu K. and Nayfeh J. (1992): *Hydromagnetic flow of a dusty fluid over a stretching sheet.* – Int. J. Nonlinear Mech., vol.27, pp.937-945.

[4] Cortell R. (2006): *Effects of viscous dissipation and work done by deformation on the MHD flow and heat transfer of a viscoelastic fluid over a stretching sheet.* – Phys. Lett. A, vol.357, pp.298-305.

[5] Ishak A., Nazar R. and Pop I. (2008): *Hydromagnetic flow and heat transfer adjacent to a stretching vertical sheet.* – Heat Mass Transf., vol.44, pp.921-927.

[6] Chien-Hsin Chen (2009): *Magneto-hydrodynamic mixed convection of a power-law fluid past a stretching surface in the presence of thermal radiation and internal heat generation/absorption.* – Int. J. Non Linear Mech., vol.44, pp.596-603.

[7] Prasad K.V., Vajravelu K. and Datti P.S. (2010): *The effects of variable fluid properties on the hydromagnetic flow and heat transfer over a non-linearly stretching sheet*. – Int. J. Ther. Sci., vol.49, pp.603-610.

[8] Elbashbeshy E.M.A. and Aldawody D.A. (2011): *Effects of thermal radiation and magnetic field on unsteady mixed convection flow and heat transfer over a porous stretching surface in the presence of internal heat generation/absorption*. – Int. J. Phy. Sci., vol.6, pp.1540-1548.

[9] Sweet E., Vajravelu K., Van Gorder R.A. and Pop I. (2011): *Analytical solution for the unsteady MHD flow of a viscous fluid between moving parallel plates*. – Commun. Non-Linear Sci. Numer. Simul., vol.16, pp.266-273.

[10] Abbasbandy S., Naz R., Hayat T. and Alsaedi A. (2014): *Numerical and analytical solutions for Falkner–Skan flow of MHD Maxwell fluid*. – Applied Mathematics and Computation, vol.242, pp.569-575.

[11] Prasad K.V., Vaidya H. and Vajravelu K. (2015): *MHD mixed convection heat transfer in a vertical channel with temperature-dependent transport properties*. – Journal of Applied Fluid Mechanics, vol.8, No.4, pp.693-701.

[12] Chambre P.L. and Young J.D. (1958): *On diffusion of a chemically reactive species in a laminar boundary layer flow*. – Phys. Fluids, vol.1, pp.48-54.

[13] Das U.N., Deka R. and Soundalgekar V.M. (1994): *Effect of mass transfer on flow past an impulsively started infinite vertical plate with constant heat flux and chemical reaction*. – Forsch. Ingenieurwes., vol.60, pp.284-287.

[14] Prasad K.V., Abel S. and Datti P.S. (2003): *Diffusion of electrically reactive species of a non-Newtonian fluid immersed in a porous medium over a stretching sheet*. – Internat. J. Non-Linear Mech., vol.38, pp.651.

[15] Akyildiz F.T., Bellout H. and Vajravelu K. (2006): *Diffusion of chemically reactive species in a porous medium over a stretching sheet*. – J. Math. Anal. Appl., vol.320, pp.322-339.

[16] Chamkha A.J., Aly A.M. and Mansour M.A. (2010): *Similarity solution for unsteady heat and mass transfer from a stretching surface embedded in a porous medium with suction/ injection and chemical reaction effects*. – Chem. Eng. Commun., vol.197, pp.846–858.

[17] Vajravelu K., Prasad K.V., Sujatha A. and Chiu-On N.G. (2012): *MHD flow and mass transfer of chemically reactive upper convected Maxwell (UCM) fluid past porous surface*. – Appl. Math. Mech. -Engl. Ed., vol.33, No.7, pp.1-12.

[18] Mabood F., Khan W.A. and Md. Ismail A.I. (2015): *MHD stagnation point flow and heat transfer impinging on stretching sheet with chemical reaction and transpiratio*n. – Chemical Engineering Journal, vol.273, pp.430-437.

[19] Lin H.T. and Shih Y.P. (1980): *Laminar boundary layer heat transfer along static and moving cylinders*. – Journal of the Chinese Institute of Engineers, vol.3, pp.73-79.

[20] Lin H.T. and Shih Y.P. (1981): *Buoyancy effects on the laminar boundary layer heat transfer along vertically moving cylinders*. – Journal of the Chinese Institute of Engineers, vol.4, pp.47-51.

[21] Ganesan P. and Loganathan P. (2001): *Unsteady natural convective flow past a moving vertical cylinder with heat and mass transfer*. – Heat and Mass Transf. Phys., vol.79, pp.73-78.

[22] Bachok N. and Ishak A. (2009): *Mixed convection boundary layer flow over a permeable vertical cylinder with prescribed surface heat flux*. – Euro. J. Sci. Res., vol.34, pp.46-54.

[23] Bachok N. and Ishak A. (2010): *Flow and heat transfer over a stretching cylinder with prescribed surface heat flux*. – Malaysian J. Math. Sci., vol.4, pp.159-169.

[24] Vajravelu K., Prasad K.V. and Santhi S.R. (2012): *Axisymmetric magneto-hydrodynamic (MHD) flow and heat transfer at a non-isothermal stretching cylinder*. – Applied Mathematics and Computation, vol.219, pp.3993-4005.

[25] Hayat T., Anwar M.S., Farooq M. and Alsaedi A. (2015): *Mixed Convection Flow of Viscoelastic Fluid by a Stretching Cylinder with Heat Transfer.* – PLoS ONE 10(3): e0118815. doi: 10.1371/journal.

[26] Rekha R.R. and Naseem Ahmed (2012): *Boundary layer flow past a stretching cylinder and heat transfer with variable thermal conductivity*. – Appl. Math., vol.3, pp.205-209.

[27] Abramowitz M. and Stegun I.A. (1965): *Handbook of Mathematical Functions*. – New York: Dover.

[28] Cebeci T. and Bradshaw P. (1984): *Physical and computational aspects of convective heat transfer*. – NewYork: Springer-Verlag.

[29] Keller H.B. (1978): *Numerical methods in boundary-layer theory*. – Annual Review of Fluid Mechanics, vol.10, pp.417-433.

[30] Vajravelu K. and Prasad K.V. (2014): *Keller-box method and its application* (HEP and Walter De Gruyter GmbH, Berlin/Boston).

[31] Grubka L.J. and Bobba K.M. (1985): *Heat transfer characteristics of a continuous stretching surface with variable temperature*. – J. Heat Transf., vol.107, pp.248-250.

[32] Ali M.E. (1994): *Heat transfer characteristics of a continuous stretching surface*. – Heat Mass Transf., vol.29, pp.227-234.

[33] Ishak A., Nazar R. and Pop I. (2009): *Boundary layer flow and heat transfer over an unsteady stretching vertical surface*. – Meccanica, vol.44, pp.369-375.

Received: 24 May, 2014

Revised: January 15, 2016